RSC Advances

PAPER

View Article Online
View Journal | View Issue

Cite this: *RSC Adv.*, 2025, **15**, 10453

A novel boronic acid-based fluorescent sensor for the selective detection of L-lysine in food samples and cells†

Wei Gao,[a] Jing Su,[a] Huarui Yang,[a] Xuefeng Zhao,[a] Jingjing Liu,[a] Zhijun Wang*[a] and Qingming Wang*[b]

Received 26th January 2025
Accepted 20th March 2025

DOI: 10.1039/d5ra00621j

rsc.li/rsc-advances

A novel probe **DFC** (2-(dicyanomethylene)-2,5-dihydro-5,5-dimethyl-4-((*E*)-2-(5-(4,4,5,5-tetramethyl-1,3,2-dioxaborolan-2-yl)furan-2-yl)vinyl)furan-3-carbonitrile) was successfully designed and synthesized for the detection of L-lysine (L-Lys). The sensing behavior was characterized using absorption and fluorescence emission spectra. Upon addition of L-Lys to **DFC**, a rapid response time of 5 seconds was observed, accompanied by a significant 4-fold enhancement in fluorescence intensity. Additionally, **DFC** exhibits an impressively low detection limit of 0.14 μMol L^{-1}. Furthermore, the applicability of **DFC** was demonstrated through successful detection of L-Lys in water samples, food samples, and imaging of L-lys in live HeLa cells.

Introduction

As one of the most abundant natural amino acids, L-Lysine (L-Lys) plays important roles in cell division, gene regulation, immune system regulation, metabolic function and so on.[1–3] The human body's requirement for L-Lys can be met by two methods: dietary intake and *in vivo* synthesis. For instance, it could be produced by the Krebs–Henseleit cycle and the gluconeogenesis cycle in metabolisms.[4–6] Due to its role in metabolisms, hyperlysinemia or cystinuria could be caused by the abnormal concentration of L-Lys.[7,8] It has also been reported that excessive intake of L-Lys may lead to metabolic disorders and obesity.[9] Therefore, it is very necessary to develop a simple, highly selective and sensitive, rapid-response method for the detection of L-Lys.

The methods of electrochemistry,[10] high-performance liquid chromatography,[9] mass spectrometry,[11] capillary electrophoresis,[12] and Fourier transform infrared spectroscopy[13] (FT-IR) have been used for the detection of L-Lys. However, the drawbacks of these methods bring many inconveniences. Fluorescence sensors have attracted much attention due to their simplicity, ease of use, high sensitivity and selectivity. Up to now, some types of sensors on the basis of different fluorophores or materials have been reported for L-Lys.[14–21] Some of these sensors exhibit insufficient selectivity for Lys due to the interference from arginine, histidine, metal ions, anions and so on.[1,14–16,18] Lysine is a strong alkaline amino acid with a isoelectric point (pI) value of 9.47.[22] Reports showed that L-Lys practically worked as a strong base to deprotonate sensors and promote the equilibrium towards the anionic.[16]

This work describe a L-Lys probe (*E*)-2-(3-cyano-5,5-dimethyl-4-(2-(5-(4,4,5,5-tetramethyl-1,3,2-dioxaborolan-2-yl)furan-2-yl) vinyl)furan-2(5*H*)-ylidene)malononitrile, that can be synthesized through straightforward organic synthesis procedures for the detection of lysine (Scheme 1). Interestingly, a distinguished color change from colorless to blue was observed with the addition of L-Lys to the **DFC** solution. A rapid fluorescence color change for **DFC** in PBS (pH = 7.40, 10 mM) was found within 5 s in the presence of L-Lys. The calculated limit of detection (LOD) of **DFC** was 0.14 μMol L^{-1}. The mechanism was proved that the hydroxyl oxygen of –COOH in L-Lys could react with the B atom of **DFC** by nucleophilic attack to form borate esters, and then aromatization of O on the furan ring with $-NH_2$ in L-Lys *via* intra-ring heteroatom substitution reaction to form a stable ring with six members. The ε-NH_2 of L-Lys and the cyanide groups formed a stable internal salt structure. The deprotonation and complexation mechanism was consistent with the previous reports.[23] Moreover, **DFC** was applied for the detection of L-Lys in real water samples and food; the results were in agreement with the L-Lysine Detection Kit (48 Assay). The cell imaging indicated that **DFC** could penetrate the cell membrane to detect the L-Lys.

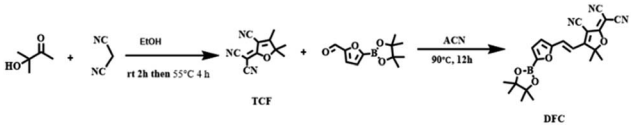

Scheme 1 Synthesis of **DFC**.

[a]*Department of Chemistry, Changzhi University, Changzhi 046011, People's Republic of China*

[b]*School of Pharmacy, Yancheng Teachers' University, Yancheng 224051, People's Republic of China*

† Electronic supplementary information (ESI) available. See DOI: https://doi.org/10.1039/d5ra00621j

Experimental section

Materials

The amino acids such as lysine (Lys), glycine (Gly), proline (Pro), Tyr, arginine (Arg), glutamine (Gln), cysteine (Cys), methionine (Met), valine (Val), phenylalanine (Phe), histidine (His), glutamic acid (Glu), threonine (Thr), aspartic acid (Asp), alanine (Ala), dipeptide such as glutathione (GSH), metal ions and anions were obtained from commercial suppliers (Shanghai Titan Scientific Co.,Ltd). All of the materials were analytical grade and used without additional purification.

Instruments

The NMR was recorded on a Bruker DRX 400 spectrometer with TMS as the internal standard and chemical shifts were expressed in ppm. HR-MS was performed with a Triple TOF TM 5600+ system. The UV-visible absorption spectrum was carried out from UV-1800 ENG 240 V. Fluorescence spectra data were recorded on an CRT-960 fluorescence spectrophotometer with a quartz cuvette (path length = 1 cm). Bioimaging of probe **DFC** with L-Lys was performed on a confocal laser scanning microscope L700 with HeLa cells.

Spectral measurements

In order to record the UV-vis spectrum, stock solution of the **DFC** (25 μMol L^{-1}) (DFC stock solution was obtained by dissolving it in DMSO, the final concentration: 10^{-2} mol L^{-1}) was prepared in PBS (pH = 7.40, 10 mM), 5 μL of L-Lys was gradually added to **DFC**, then the UV-Vis spectra were monitored.

To record fluorescence spectra, the stock solution of **DFC** and the L-Lys were prepared as the same as that used for UV-vis method. 25 μmol L^{-1} **DFC** was added to 2 mL PBS (pH = 7.40, 10 mM), then 2 μL of 10^{-3} mol per L-Lys was gradually added, then the fluorescence spectra were recorded. The excitation wavelength was 380 nm and the emission wavelength were collected at 390–650 nm. The slit widths were 5/5 nm.

Food sample treatment

8.0 g of cashew nuts, soybeans, red beans, millet, flour, mung beans, black beans were all purchased from local supermarkets (Yonghui, Changzhi). Pre-treatment of the food samples were done before the experiment by crushing the food samples into pieces and passing through a 60 mesh sieve. The samples were put in round bottom flasks, add petroleum ether and soak with stir continuously for 48 hours. And then degrease, dry and dissolve in anhydrous ethanol. At last, distilled water was added to reach 50 mL. The supernatant was centrifuged for the measurement of the concentration of L-Lys.

Cell culture and imaging

Cell culture. HeLa cells were cultured in Dulbecco's Modified Eagle Medium (DMEM) supplemented with 100 U per mL penicillin, 10% fetal bovine serum (FBS), and 100 μg per mL streptomycin. Cells were maintained in a humidified incubator set at 37 °C with 5% CO_2. HeLa cells were seeded in 96-well plates at a density of 8000 cells per well and cultured for 24 hours to facilitate cellular adherence. Subsequently, cells were exposed to various concentrations of **DFC** (0.0, 20.0, 40.0, 60.0, and 80.0 μmol L^{-1}) for an additional 24 hours. After treatment, the medium was carefully aspirated, and 110 μL of fresh medium containing 10 μL of CCK-8 reagent was added to each well under light-protected conditions. The plates were then incubated for 20 min before absorbance was measured at 450 nm using a microplate reader to evaluate cytotoxicity.

Fluorescence confocal imaging

For the imaging experiment, HeLa cells at a density of 30 000 cells per well in laser confocal culture dishes (diameter: 35 mm; glass bottom diameter: 10 mm) were incubated with 20.0 μmol L^{-1} **DFC** at 37 °C for 20 minutes prior to laser confocal imaging. To determine the effect of exogenous Lys, HeLa cells pre-incubated with 20.0 μmol L^{-1} **DFC** were washed thoroughly and subsequently incubated with Lys (20.0, 30.0, 40.0 and 50.0 μmol L^{-1}) for 20 minutes before undergoing laser confocal imaging. All cells were washed three times with sterile PBS and imaged using an confocal laser scanning microscope L700 (excitation wavelength = 405 nm, emission collection range = 450–500 nm).

Synthesis of DFC

Synthesis of 2-(3-cyano-4,5,5-trimethylfuran-2(5*H*)-ylidene) malononitrile (TCF). TCF was synthesized in accordance with the methodologies detailed in the referenced literature.[24] A mixture of sodium ethoxide (0.45 mmol), 3-hydroxy-3-methyl-2-butanone (0.306 g, 3 mmol), and malononitril (0.396 g, 6 mmol) in a 100 mL round-bottom flask were dissolved in ethanol (10 mL), the solution was stirred at room temperature for 2 hours. And then, 30 mL of ethanol were added and the reactants continue to react at 55 °C for 4 hours. After the reaction is over, the mixture cooled to room temperature. The solid precipitate was filtered and washed with a small amount of cold ethanol to give off-white crystals.

Synthesis of 2-(3-cyano-5,5-dimethyl-4-(2-(5-(4,4,5,5-tetramethyl-1,3,2-dioxaborolan-2-yl)furan-2-yl)vinyl)furan-2(5*H*)-ylidene)malononitrile. DFC was synthesized in accordance with the methodologies detailed in the referenced literature.[25] **TCF** (0.0812 g, 0.4 mmol) and 5-(4,4,5,5-tetramethyl-1,3,2-dioxaborolan-2-yl) furan-2-carbaldehyde (0.0727 g, 0.33 mmol) were dissolved in acetonitrile (30 mL) in a 100 mL round-bottom flask equipped with a reflux condenser, the solution was subsequently stirred at 90 °C for 12 h under nitrogen protection. After the reaction, most of the solvent was removed under reduced pressure. Dimethyl ether (70 mL) was added to the residue and the resulting solid precipitates was filtered and washed with a small amount of ether to give orange solid. MS (ESI): *m*/*z* calc. for $C_{22}H_{22}BN_3O_4$: 403.2450; found: 404.1798 $[M + H]^+$.

Results and discussion

Detection of L-Lys in solution

The spectroscopic response of **DFC** to L-Lys was investigated. As shown in Fig. S2,† probe **DFC** exhibited a strong absorption at

310 nm and a noticeable emission peak at 560 nm, with a Stokes shift of 250 nm. The absorption of DFC at 310 nm was enhanced with the addition of L-Lys (Fig.S3†). At the same time, the emission peak of **DFC** shifted from 560 nm to 450 nm (about 110 nm).

Fig. 1a showed the optical response between **DFC** and L-Lys in PBS (pH = 7.40, 10 mM). When L-Lys was added to the solution of **DFC**, an emission peak at 450 nm appeared. And its intensity was gradually enhanced with the increasing of L-Lys. The fluorescence intensity was enhanced about 3.79-fold when 24 μMol L^{-1} of L-Lys was added. The color of the solution changed from colorless to blue under a 365 nm UV lamp. Furthermore, the UV-vis titration was used to investigate the quantitative response of **DFC** to L-Lys. As depicted in Fig. S4,† with the increase of L-Lys (0–37.5 μMol L^{-1}), the peak at 310 nm was gradually increased. Meantime, a weak band at 503 nm remained unchanged. These changes indicated that a reaction was occurred between **DFC** and L-Lys. Most importantly, the emission intensity of **DFC** at 450 nm showed excellent linearity with L-Lys concentrations increased from 0 to 50 μMol L^{-1}. The equation of F_{450nm} and [L-Lys] was plotted as $Y = 23.475 + 3.322X$ with a correlation coefficient (R^2) value of 0.99945, indicating that **DFC** could be used in actual sample testing (Fig. 1b). Accordingly, the detection limit was calculated as 0.15 μMol L^{-1}, which is lower than most reported methods.[26–29]

In order to optimise the detection conditions, time and pH were evaluated on the fluorescence intensity of the **DFC** response to L-Lys. Firstly, the effect of time on the detection capability for L-Lys was investigated. The results showed that the **DFC** showed a negligible variation during the assay time (1 h). After the addition of L-Lys, the fluorescence intensity of **DFC** increased rapidly and it took about 5 s to reach the maximum value, and the maximum value was maintained unchanged within the assay time (1 h). The effect of different concentrations (10, 25 μMol L^{-1}) of L-Lys on the reaction time was investigated and it was found that the concentration of L-Lys had no effect on the time.

To explore the impact of pH on the detection of L-Lys, we assessed the pH responses of the fluorescence intensities of DFC and the mixture of DFC and L-Lys. As shown in Fig. 2b, **DFC** showed a very low level of fluorescence intensity under the pH of 4.00, 6.86, 7.40, 9.18, 10.01. When L-Lys was induced, the fluorescence intensity of **DFC** was remarkably enhanced. The enhancement was 3.39-fold, 4.37-fold, 4.02-fold, 3.67-fold and 3.71-fold at pH = 4.00, 6.86, 7.40, 9.18, 10.01 respectively. A wide pH range of 4.0–10.0 for **DFC** response to L-Lys was similar to the early reports.[20,30]

Selectivity

To evaluate the specificity of **DFC** for L-Lys, a large number of related species such as amino acids (Gly, Pro, Tyr, Arg, Gln, Cys, Met, Val, Phe, His, Glu, Thr, Asp, Ala, GSH), anions (CO_3^{2-}, SO_4^{2-}, SO_3^{2-}, ACO^-, HSO_4^-, $H_2PO_4^-$, $S_2O_3^{2-}$, HCO_3^-, Cl^-, HSO_3^-, PO_4^{3-}, NO_3^-, F^-, S^{2-}, ClO^-) and metal ions (Na^+, K^+, Mg^{2+}, Fe^{3+}, Ca^{2+}, Al^{3+}, Zn^{2+}, Cr^{3+}, Cu^{2+}, Ni^{2+}, Cd^{2+}, Mn^{2+}) were tested (as showed in Fig. S5†). The results showed that only L-Lys could enhance the fluorescence intensity of **DFC** in PBS (pH =

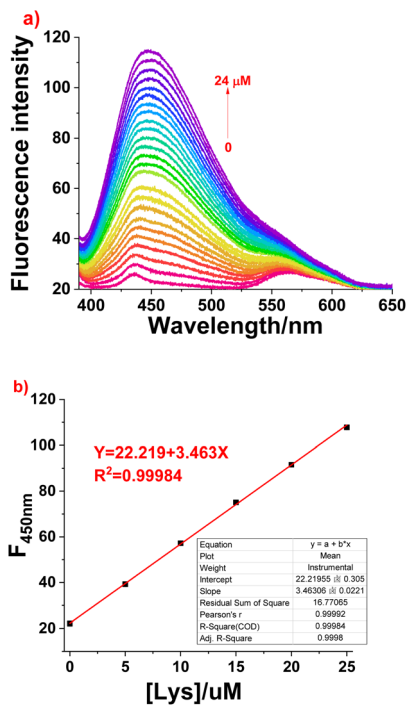

Fig. 1 (a) Fluorescence spectral response of DFC (25 μMol L^{-1}) with titration of various concentrations of L-Lys (0–24 μMol L^{-1}, λ_{ex} = 380 nm). Inset: emission change. (b) The linear relationship between the fluorescence intensity ratio (F_{450nm}) of DFC and L-Lys concentrations (0–50 μMol L^{-1}), n = 3.

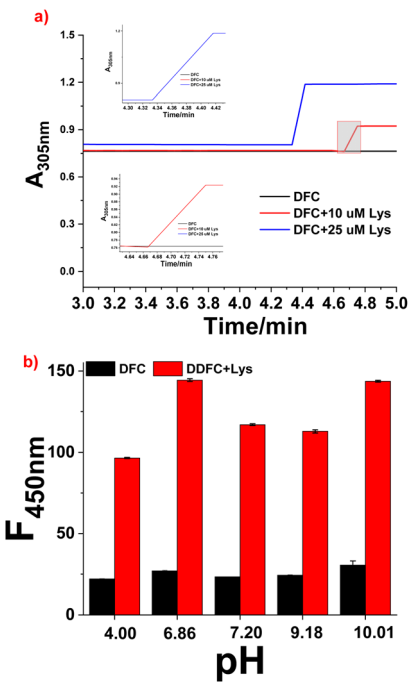

Fig. 2 (a) The time dependence of **DFC** (25 μMol L^{-1}) in the absence and presence of L-Lys (10, 25 μMol L^{-1}) in PBS (pH = 7.40, 10 mM). (b) The pH-dependent responses of **DFC** to L-Lys at 450 nm, λ_{ex} = 380 nm, n = 3.

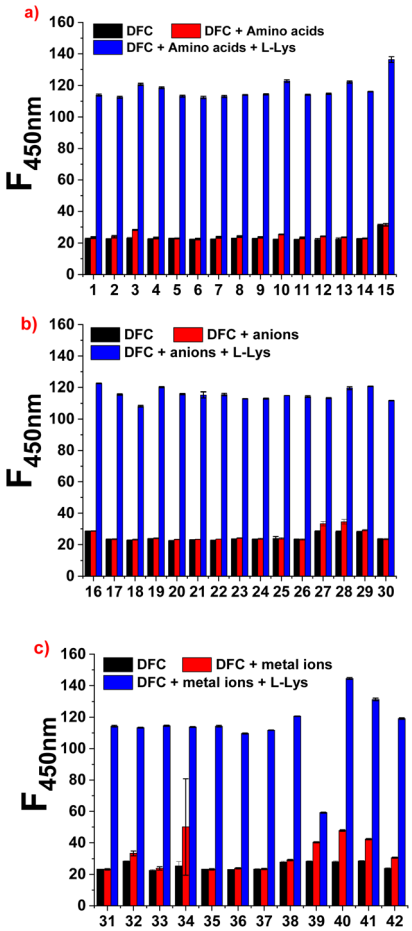

Fig. 3 Fluorescence intensity (F_{450nm}) of **DFC** (25 μMol L^{-1}) in response to L-Lys (100 μMol L^{-1}) after adding a variety of (a) amino acids (500 μMol L^{-1}), (b) anions (500 μMol L^{-1}), (c) metal ions (500 μMol L^{-1}). (1) Gly; (2) Pro; (3) Tyr; (4) Arg; (5) Gln; (6) Cys; (7) Met; (8) Val; (9) Phe; (10) His; (11) Glu; (12) Thr; (13) Asp; (14) Ala; (15) GSH; (16) CO_3^{2-}; (17) SO_4^{2-}; (18) SO_3^{2-}; (19) ACO^-; (20) HSO_4^-; (21) $H_2PO_4^-$; (22) $S_2O_3^{2-}$; (23) HCO_3^-; (24) Cl^-; (25) HSO_3^-; (26) PO_4^{3-}; (27) NO_3^-; (28) F^-; (29) S^{2-}; (30) ClO^-; (31) Na^+; (32) K^+; (33) Mg^{2+}; (34) Fe^{3+}; (35) Ca^{2+}; (36) Al^{3+}; (37) Zn^{2+}; (38) Cr^{3+}; (39) Cu^{2+}; (40) Ni^{2+}; (41) Cd^{2+}; (42) Mn^{2+}, $n = 3$.

7.40,10 mM), no obvious fluorescence changes were obtained in the presence of other related species. In addition, we investigated whether other related species coexisting with L-Lys could enhance the fluorescence intensity of **DFC** or not. From Fig. 3, when **DFC** (25 μMol L^{-1}) in PBS (pH = 7.40,10 mM) was first treated with 500 μMol L^{-1} of amino acids, anions and metal ions, the fluorescence intensity of **DFC** was almost unchanged, and the fluorescence was turned on when 100 μMol L^{-1} of L-Lys was added to the above system. These results told us that the specific recognition of **DFC** for L-Lys was not affected by amino acids, anions and metal ions, and that **DFC** could be used for L-Lys in biological and food samples.

Sensing mechanism

The sensing mechanism between **DFC** and L-Lys has been proposed in Scheme 2. Since the hydroxyl oxygen of –COOH in L-Lys could react with the B atom of **DFC** by nucleophilic attack to form borate esters. Aromatization of O on the furan ring with $–NH_2$ in L-Lys *via* intra-ring heteroatom substitution reaction.[31] The ε-NH_2 of L-Lys and the cyanide groups formed a stable internal salt structure.[20] The pyrrole 2-position C–C and 2 H-furan 2-position C–C cannot rotate, resulting in increased fluorescence intensity of **DFC**-Lys. **DFC** and L-Lys was formed a complex in 1 : 1 stoichiometry and were identified by the Job's plot study. The mechanism was confirmed by EI-MS. After mixing **DFC** with 1 equal amount of L-Lys, a peak $m/z = 531.2614$ was obtained, which could be belonging to [**DFC** + L-Lys] (Cal. 531.2653) (Fig. 4). The result was used to further verify the mechanism.

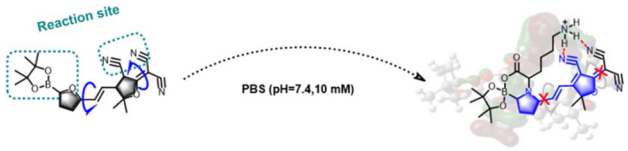

Scheme 2 The possible sensing mechanism of **DFC** for L-Lys.

Density Functional Theory (DFT) calculations were performed at the ωb97xd/6-31g(d) level on the reaction of **DFC** (**1**) and L-Lys (**2**) to further clarify the sensing mechanism.[32] Due to the alkalinity of the ε-amino group in L-Lys is strong, so it can capture the carboxyl group proton on L-Lys to form the compound **3**. From Fig. 5, the compound **4** was formed between compound **3** and **1** by the heteroatom substitution reaction of aromatisation O on the furan ring with $–NH_2$ in **2**. The reaction energy (ΔG) of this reaction is −62.3 kcal mol^{-1}, which is an exothermic reaction. Compound **5** was obtained by a ring–closing reaction with the reaction energy of −15.4 kcal mol^{-1}. Moreover, the HOMO-52 and HOMO-56 of structure **5** show that hydrogen bonds are existed between the H atom of the ε-amino group on L-Lys and the N atom of the cyano group on **DFC**. **DFT** further validated our proposed mechanism.

Determination of L-Lys in different water samples

We then investigated the application of **DFC** in tracing the concentration of L-Lys in real samples.[33,34] A certain amount of L-Lys was dissolved in river water, purified water and tap water. The fluorescence intensity of **DFC** (25 μMol L^{-1}) with various

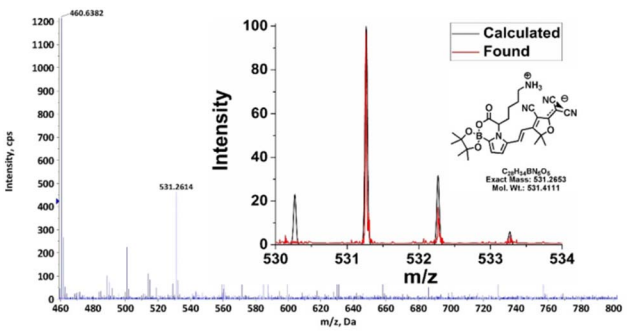

Fig. 4 ESI mass spectrum of **DFC** upon addition of L-Lys.

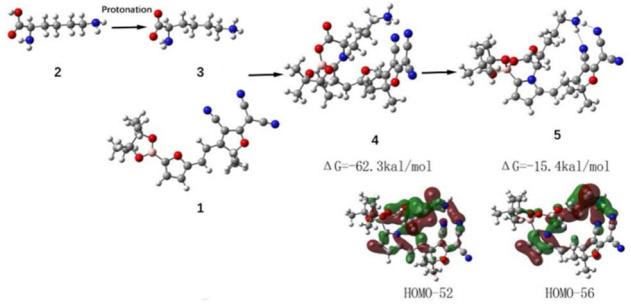

Fig. 5 Density functional theory (DFT) calculations on the reaction of DFC and L-Lys.

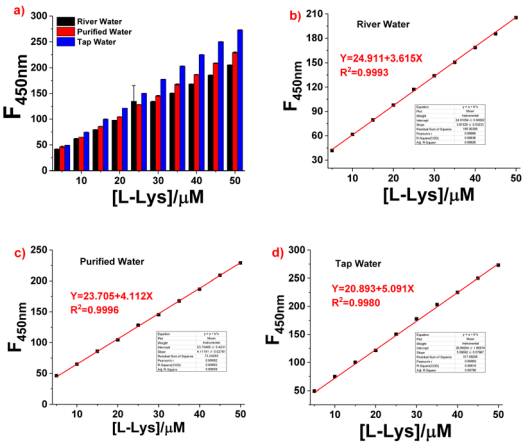

Fig. 6 (a) Fluorescence intensity of DFC in the presence of L-Lys (5, 10, 15, 20, 25, 30, 35, 40, 45, 50 μMol L^{-1}) in three water samples. Plots of fluorescence intensity at F_{450nm} *vs.* L-Lys concentration (5–50 μMol L^{-1}) in (b) river water and (c) purified water and (d) tap water samples, $n = 3$.

concentrations (5, 10, 15, 20, 25, 30, 35, 40, 45, 50 μMol L^{-1}) of L-Lys was investigated in these real samples. From Fig. 6, a good linear relationship between [L-Lys] and F450 nm, and the linear correlation coefficients for river water, purified water and tap water were 0.9990, 0.99963 and 0.99936, respectively. The recoveries of **DFC** for the detection of L-Lys ranged from 96.4% to 112% (Table 1). The good recoveries showed that **DFC** could be used for the detection of L-Lys in real water samples.

Determination of L-Lys in food samples

There is an abundance of amino acids in food. So we chose commercially available food samples to realize the detection of L-Lys.

Three parallel experiments were carried out in accordance with the experimental method, and the relative standard deviation and the recovery were calculated. The experiment was carried out three times in parallel. From Table 2, the contents in cashew nuts, soybeans, red beans, millet, flour, mung beans, black beans were different from each other. The content of L-Lys in these seven samples were 1.68, 2.65, 1.37, 0.20, -, 1.92, and 0.09 mg g^{-1}, respectively, measured by **DFC** in PBS (pH = 7.40, 10 mM). To verify the accuracy of the method proposed in this

Table 1 Response data of probe DFC to L-Lys in different samples ($n = 3$)

Sample	Added (μmol L^{-1})	Detected (μmol L^{-1})	Recovery (%)
River water	5	5.39 ± 0.07	108
	10	10.58 ± 0.02	106
	15	15.16 ± 0.07	101
	20	19.37 ± 0.06	96.8
	25	25.19 ± 0.07	105
	30	30.27 ± 0.26	101
	35	35.27 ± 0.06	101
	40	40.65 ± 0.11	102
	45	45.35 ± 0.15	101
	50	49.84 ± 0.28	99.7
Purified water	5	4.82 ± 0.07	96.4
	10	10.23 ± 0.17	102
	15	15.76 ± 0.09	105
	20	19.85 ± 0.10	99.3
	25	25.53 ± 0.09	102
	30	30.66 ± 0.28	102
	35	34.58 ± 0.31	98.8
	40	40.11 ± 0.15	100
	45	46.61 ± 0.19	104
	50	50.68 ± 0.05	101
Tap water	5	5.60 ± 0.01	112
	10	10.20 ± 0.36	102
	15	16.45 ± 0.17	110
	20	20.44 ± 0.03	102
	25	26.13 ± 0.06	105
	30	31.37 ± 0.16	105
	35	36.06 ± 0.20	103
	40	39.80 ± 0.26	99.5
	45	47.11 ± 0.23	105
	50	51.11 ± 0.17	102

Table 2 Detection of L-lysine in different samples by the DFC and L-lysine detection kit (48 assay) ($n = 3$)

Samples	L-Lysine detection kit (mg g^{-1})	RSD%	DFC (mg g^{-1})	RSD%
Cashew nuts	1.53	0.223	1.68	3.17
Soybeans	2.60	0	2.65	1.04
Red beans	1.22	0.402	1.37	5.59
Millet	0.06	0	0.20	1.16
Flour	0.26	0	—	—
Mung beans	1.90	0.112	1.92	3.09
Black beans	0.04	0.112	0.09	0.79

paper, the L-Lysine Detection Kit (48 Assay) was used to further validate the L-Lys. The results calculated by the L-Lysine Detection Kit (48 Assay) showed that the L-Lys in these seven samples were 1.53, 2.60, 1.22, 0.06, 0.26, 1.90, and 0.04 mg g^{-1}, respectively. A comparison of the DFC and L-Lysine Detection Kit (48 Assay) methods showed that the two methods were consistent with each other.

Imaging of L-Lys in living cells

In order to expand the application of **DFC**, cellular fluorescence imaging for **DFC** was conducted through HeLa cells. First, from

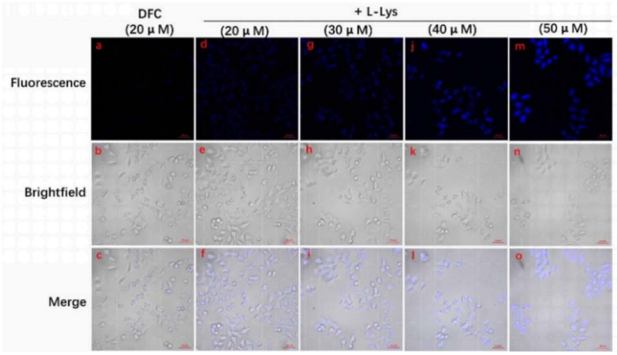

Fig. 7 Fluorescence microscopy images of HeLa cells. (a)–(c) HeLa cells incubated with **DFC** (20 μMol L^{-1}) for 20 min. (d)–(f) HeLa cells pretreated with **DFC** (20 μMol L^{-1}) and then treated with L-Lys (20 μMol L^{-1}) for 20 min. (g)–(i) HeLa cells pretreated with **DFC** (20 μMol L^{-1}) and then treated with L-Lys (30 μMol L^{-1}) for 20 min. (j)–(l) HeLa cells pretreated with **DFC** (20 μMol L^{-1}) and then treated with L-Lys (40 μMol L^{-1}) for 20 min. (m)–(o) HeLa cells pretreated with **DFC** (40 μMol L^{-1}) and then treated with L-Lys (50 μMol L^{-1}) for 20 min.

Fig. S6,† the minimal cytotoxicity of **DFC** toward HeLa cells was confirmed by the cytotoxicity experiments, and showed the high concentration was 80 μMol L^{-1} (84.2% cell viability). We used the **DFC**, which has good biocompatibility and low toxicity, for cellular fluorescence imaging. From Fig. 7, we could find that when the cells were stained with **DFC** (20 μMol L^{-1}), and further treated with L-Lys (0, 20, 30, 40, 50 μM), a visible variation of fluorescence intensity was found. Moreover, the blue fluorescence in HeLa cells became strong with the increase of the L-Lys. The cell imaging indicated that **DFC** could penetrate the cell membrane to detect the L-Lys.

Conclusions

A simple and efficient "turn-on" fluorescence sensor was developed for the highly sensitive and selective detection of L-Lys. The addition of L-Lys to the solution of **DFC** in PBS (pH = 7.42, 10 mM) induced a marked fluorescence enhancement (3.79-fold). No significant changes in fluorescence emission or colour were observed when the other amino acids (Gly, Pro, Tyr, Arg, Gln, Cys, Met, Val, Phe, His, Glu, Thr, Asp, Ala), metal ions, anions and GSH were added to **DFC**. The detection limit of **DFC** for Lys was 0.15 μMol L^{-1} based on fluorescence titration and **DFC** showed high stability for L-Lys in the pH range of 4.00 to 10.01. **DFC** was used to detect L-Lys in various water samples with recoveries ranging from 96.4% to 112%. Furthermore, the comparison of the **DFC** and L-Lysine Detection Kit (48 Assay) methods showed that the two methods were in agreement with each other. In addition, cellular experiments demonstrated that **DFC** has low toxicity and high penetration, which could be used for fluorescence imaging in HeLa cells.

Data availability

The data supporting this article have been included as part of the ESI.†

Author contributions

The manuscript was written through contributions of all authors. All authors have given approval to the final version of the manuscript.

Conflicts of interest

There are no conflicts to declare.

Acknowledgements

This work was supported by the Scientific and Technological Innovation Programs of Higher Education Institutions in Shanxi (No. 2023L334); The special fund for Science and Technology Innovation Teams of Shanxi Province (202204051001034); Fund for Shanxi "1331 Project", Horizontal Project from Shanxi Agricultural University (Shanxi Academy of Agricultural Sciences) Millet Research Institute (HX0608) and the applied teaching material construction project of Changzhi University (XN0329).

Notes and references

1 L. Wang, Z. L. Wei, C. Liu, W. K. Dong and J. X. Ru, *Spectrochim. Acta, Part A*, 2020, **239**, 118496.
2 A. Chéramy, M. L'Hirondel, G. Godeheu, F. Artaud and J. Glowinski, *Amino Acids*, 1998, **14**, 63–68.
3 J. Hao, M. Wang, S. Wang, Y. Huang and D. Cao, *Dyes Pigm.*, 2020, **175**, 108131.
4 A. M. Pettiwala and P. K. Singh, *Spectrochim. Acta, Part A*, 2018, **188**, 120–126.
5 H. Yoshida, Y. Nakano, K. Koiso, H. Nohta, J. Ishida and M. Yamaguchi, *Anal. Sci.*, 2001, **17**, 107–112.
6 Y. Zhou, J. Won, J. Y. Lee and J. Yoon, *Chem. Commun.*, 2011, **47**, 1997–1999.
7 S. Lohar, D. A. Safin, A. Sengupta, A. Chattopadhyay, J. S. Matalobos, M. G. Babashkina, K. Robeyns, M. P. Mitoraj, P. Kubisiak, Y. Garcia and D. Das, *Chem. Commun.*, 2015, **51**, 8536–8539.
8 P. Felig, *Annu. Rev. Biochem.*, 1975, **44**, 933–955.
9 G. Wu, *Amino Acids*, 2009, **37**, 1–17.
10 G. L. Luque, N. F. Ferreyra and G. A. Rivas, *Talanta*, 2007, **71**, 1282–1287.
11 N. Burford, M. D. Eelman, D. E. Mahony and M. Morash, *Chem. Commun.*, 2003, 146–147, DOI: 10.1039/B210570E.
12 C. K. Larive, S. M. Lunte, M. Zhong, M. D. Perkins, G. S. Wilson, G. Gokulrangan, T. Williams, F. Afroz, C. Schöneich, T. S. Derrick, C. R. Middaugh and S. Bogdanowich-Knipp, *Anal. Chem.*, 1999, **71**, 389r–423r.
13 G. Yao and Q. Huang, *Spectrochim. Acta, Part A*, 2022, **278**, 121371.
14 G. Mi, M. Yang, C. Wang, B. Zhang, X. Hu, H. Hao and J. Fan, *Spectrochim. Acta, Part A*, 2021, **253**, 119555.
15 Y. F. Shi, Y. P. Jiang, P. P. Sun, K. Wang, Z. Q. Zhang, N. J. Zhu, R. Guo, Y. Y. Zhang, X. Z. Wang, Y. Y. Liu,

J. Z. Huo, X. R. Wang and B. Ding, *Spectrochim. Acta, Part A*, 2021, **249**, 119214.
16 T. Wang, Q. Pang, Z. Tong, H. Xiang and N. Xiao, *Spectrochim. Acta, Part A*, 2021, **258**, 119824.
17 S. Sudewi, C. H. Li, S. Dayalan, M. Zulfajri, P. V. S. Sashankh and G. G. Huang, *Spectrochim. Acta, Part A*, 2022, **279**, 121453.
18 S. Wei, B. wang, H. Zhang, C. Wang, S. Cui, X. Yin, C. Jiang and G. Sun, *Chem. Eng. J.*, 2023, **466**, 143103.
19 J. Wu, Y. Luo, C. Cui, Q. Han and Z. Peng, *Spectrochim. Acta, Part A*, 2024, **309**, 123840.
20 J. Yu, J. Fan, Y. Song, Y. Zhao, Z. Lin, L. Jiang and H. Li, *Spectrochim. Acta, Part A*, 2024, **308**, 123734.
21 Y. Q. Pan, X. Xu, Y. Zhang, Y. Zhang and W. K. Dong, *Spectrochim. Acta, Part A*, 2020, **229**, 117927.
22 H. X. Liu, R. S. Zhang, X. J. Yao, M. C. Liu, Z. D. Hu and B. T. Fan, *J. Chem. Inf. Comput. Sci.*, 2004, **44**, 161–167.
23 R. S. Bhosale, G. V. Shitre, R. Kumar, D. O. Biradar, S. V. Bhosale, R. Narayan and S. V. Bhosale, *Sens. Actuators, B*, 2017, **241**, 1270–1275.
24 Z. C. Wang, L. C. Yuan, Q. Zhang and D. W. Lei, CN202111296746.8, 2022.
25 A. Oehlke, A. A. Auer, K. Schreiter, N. Friebe and S. Spange, *Chem.–Eur. J.*, 2015, **21**, 17890–17896.
26 A. Borchers and T. Pieler, *Genes*, 2010, **1**, 413–426.
27 M. Zhang, J. Qiao, S. Zhang and L. Qi, *Talanta*, 2018, **182**, 595–599.
28 H. Zhao, L. Li, Y. Cao, G. Gong, Y. Zhou, X. Gao, L. Pu and G. Zhao, *Tetrahedron Lett.*, 2019, **60**, 1238–1242.
29 K. Ghosh, D. Tarafdar, I. D. Petsalakis and G. Theodorakopoulos, *Eur. J. Org Chem.*, 2017, **2017**, 355–362.
30 Z. Zhu, Y. Wang, H. Ding, C. Fan, Y. Tu, G. Liu and S. Pu, *Luminescence*, 2021, **36**, 691–697.
31 Z. Xu, P. Deng, J. Li and S. Tang, *Sens. Actuators, B*, 2018, **255**, 2095–2104.
32 M. Xing, Y. Han, Y. Zhu, Y. Sun, Y. Shan, K. N. Wang, Q. Liu, B. Dong, D. Cao and W. Lin, *Anal. Chem.*, 2022, **94**, 12836–12844.
33 T. Gao, L. Gao, J. Zhang, W. Zhou, Z. Zhang, X. Niu and T. Hu, *J. Lumin.*, 2021, **231**, 117798.
34 W. Gao, H. Song, X. Wang, X. Liu, X. Pang, Y. Zhou, B. Gao and X. Peng, *ACS Appl. Mater. Interfaces*, 2018, **10**, 1147–1154.